Iterative Detection and Decoding for Separable Two-Dimensional Intersymbol Interference

Yunxiang Wu, Joseph A. O'Sullivan, *Fellow, IEEE*, Naveen Singla, *Student Member, IEEE*, and Ronald S. Indeck, *Fellow, IEEE*

***Abstract*—We introduce two detection methods for uncoded two-dimensional (2-D) intersymbol interference (ISI) channels. The detection methods are suitable for a special case of 2-D ISI channels where the channel response is separable. In this case, the 2-D ISI is treated as the concatenation of two one-dimensional ISI channels. The first method uses equalization to reduce the ISI in one of the two dimensions followed by use of a maximum *a posteriori* (MAP) detector for the ISI in the other dimension. The second method employs modified MAP algorithms to reduce the ISI in each dimension. The implementation complexity of the two methods grows exponentially in the ISI length in either the row or column dimension. We develop two iterative decoding schemes based on these detection methods and low-density parity-check codes as error correction codes. Simulation results show that the bit-error-rate performance loss caused by the 2-D ISI for the separable channel response considered is less than 1 dB over a channel without ISI. This motivates equalizing a general 2-D ISI channel response to a nearby separable matrix.**

***Index Terms*—Equalization, iterative decoding, nonbinary MAP, turbo equalization, two-dimensional intersymbol interference.**

I. Introduction

TWO-DIMENSIONAL (2-D) intersymbol interference (ISI) arises during detection in page-oriented optical memories [1] and possibly in future magnetic recording systems. Current hard disk drives store data in concentric tracks, and since the spacing between adjacent tracks is large, the detection/decoding algorithms ignore the intertrack interference without significant performance loss. While conventional recording density is becoming saturated due to the so-called "superparamagnetic" phenomenon, great efforts have been dedicated to new magnetic recording technologies in recent years. Reducing the bit-aspect ratio is one approach to increasing recording density, but it leads to increased interference from the adjacent tracks which, taken together with the downtrack ISI, can be treated as 2-D ISI. In this paper, we propose and study the performance of iterative detection and decoding algorithms for storage media having 2-D ISI during readback. Throughout the paper, we refer to the part of the algorithms that mitigate the effects of ISI as detection. The iterations and decisions directly associated with the low-density parity-check (LDPC) codes, which are used for error correction, are referred to as decoding.

Manuscript received June 11, 2002; revised April 5, 2003. This work was supported in part by the National Science Foundation under Grants ECS-0000434 and ECS-9900159.

Y. Wu was with the Department of Electrical Engineering, Washington University, St. Louis, MO 63130-4899 USA. He is now with Samsung Information Systems America Inc., San Jose, CA 95134 USA.

J. A. O'Sullivan, N. Singla, and R. S. Indeck are with the Department of Electrical Engineering, Washington University, St. Louis, MO 63130-4899 USA (e-mail: jao@ee.wustl.edu).

Digital Object Identifier 10.1109/TMAG.2003.814291

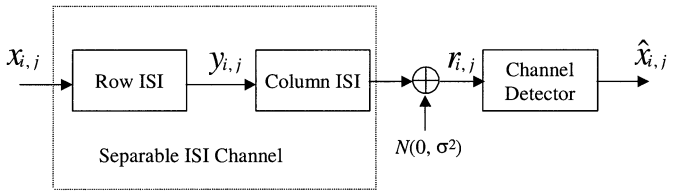

Fig. 1. A separable 2-D ISI channel is viewed as two 1-D ISI channels.

Various detection algorithms for 2-D ISI have been proposed in [1]–[4]. The detection method proposed in [2] is able to generate soft decisions for the recorded binary bits. This algorithm iteratively performs the calculation of two parts, namely, the likelihood exchange and the likelihood filtering. The calculation of the first part entails computing a set of combining coefficients. For an $L \times L$ ISI matrix, the number of the combining coefficients is exponential in L^2 [2]. Thus, it is impractical to use this method for applications where ISI spreads over a large neighborhood, for example, high-density storage media. In this paper, we propose and investigate the performance of two new detection methods that have a computational complexity proportional to the exponential of L. The underlying premise here is that the 2-D ISI matrix is separable into a product of two vectors, thus allowing us to treat the 2-D ISI as the concatenation of two one-dimensional (1-D) ISI channels, a 1-D row ISI followed by a 1-D column ISI (Fig. 1).

The first method uses equalization to reduce the ISI in one of the two dimensions followed by a maximum *a posteriori* (MAP) [5] detector for the ISI in the other dimension. When used with LDPC codes, the MAP detector and the LDPC decoder form an iterative decoder.

The second method performs detection by using an iterative detector that employs modified MAP algorithms for the ISI in each dimension. This detector is very similar to the detector of serially concatenated convolutional codes (SCCCs) [6] but for two differences. First, the trellis of the 1-D ISI in the column direction is not binary, so a MAP algorithm for nonbinary trellises needs to be employed. Second, the output of the row ISI is not observed directly, necessitating modification in the MAP algorithm. When used with LDPC codes, the iterative detector and the LDPC decoder form an iterative decoder with three constituent decoder/detectors.

While we cannot yet implement 2-D recording and reading, progress is being made in areas that provide encouragement that

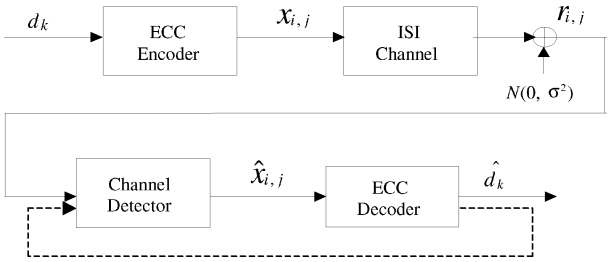

Fig. 2. System model.

we will achieve this technology in the future. Advanced media, such as patterned media, together with multitrack optical transducers or magnetic recording sensors [7], [8], promise advanced systems that could implement and fully utilize 2-D recording strategies.

The rest of the paper is organized as follows: Section II describes the system model. Section III provides a brief description of the detection methods for an uncoded 2-D ISI channel. The iterative decoding schemes are described in Section IV. Simulation results are presented in Section V, and conclusions are drawn in Section VI.

II. System Model

We assume the channel is a discrete 2-D ISI channel. The user bit d_k is encoded by an error correction code (ECC) encoder, and the encoded bits are scanned into a matrix $\mathbf{X}$ with elements $x_{i,j} \in \{\pm 1\}$. The binary level signaling may correspond to saturation recording on a magnetic medium or the absence and presence of holes on an optical medium. The output of the channel is a matrix $\mathbf{R}$ with elements

$$r_{i,j} = \sum_{k_1=0}^{L-1} \sum_{k_2=0}^{L-1} x_{i-k_1,j-k_2} h_{k_1,k_2} + n_{i,j} \tag{1}$$

where $n_{i,j}$ are realizations of a zero-mean, variance σ^2 additive white Gaussian noise (AWGN) sequence. The channel response used for our simulations is

$$h = \begin{pmatrix} 1 & 0.5 \\ 0.5 & 0.25 \end{pmatrix}. \tag{2}$$

This channel response is separable into $[1\ \ 0.5]^T \cdot [1\ \ 0.5]$. In (1), L represents the number of elements over which the ISI extends in each dimension. With the above assumptions, the recording system can be represented by a discrete-time communication system shown in Fig. 2. Anticipating the use of joint turbo decoding and equalization, the dashed line in Fig. 2 provides a path to feedback information from the decoder to the detector.

For error correction, we use LDPC coset codes [9]. Prior to transmission over the channel, a width L guard band of -1's is added around the matrix $\mathbf{X}$. The reason for using the guard band is to isolate sectors in 2-D and also to provide ISI trellis termination. To evaluate the performance of the detection methods and

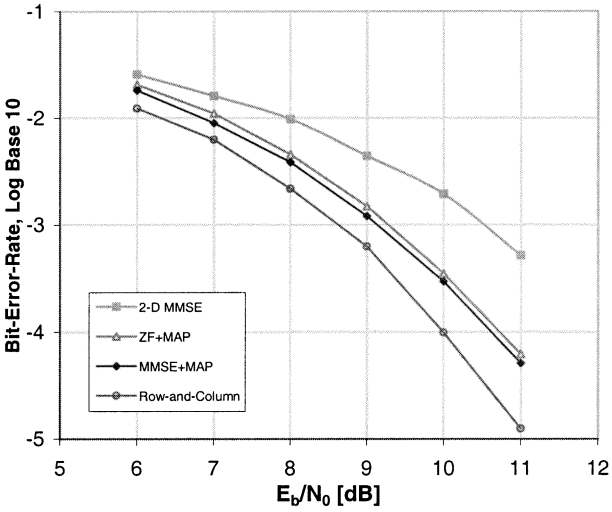

Fig. 3. Performance comparison for detection algorithms.

iterative decoding schemes, we define the signal-to-noise ratio as

$$E_b/N_0 = 10 \log_{10} \left(\frac{\sum_{i,j} h_{i,j}^2}{2C \cdot \sigma^2} \right) \tag{3}$$

where C is the code rate.

III. Detection Algorithms for 2-D ISI Channels

In this section, we describe two detection methods designed for the case when the channel response matrix is separable. For a general channel response, equalization might be considered to equalize the channel response to a nearby separable matrix. The separable matrix can be chosen with the same consideration as 1-D partial-response equalization, i.e., the spectrum of the separable matrix should be well matched to that of the 2-D ISI so that the noise is not excessively boosted by equalization. The minimum mean-squared error (MMSE) criterion might be used to design the equalizer [1].

A. Combination of Equalization and MAP Approach

This method uses equalization to reduce the ISI in one of the two dimensions. Therefore, after equalization, the 2-D ISI detection is reduced to a 1-D ISI detection problem. For the remaining ISI, a MAP detector, described in [5] and [10], is used. In this paper, zero-forcing (ZF) and MMSE criteria are used for equalization. The performance of this approach using both MMSE and ZF criterion is shown in Fig. 3. For comparison, Fig. 3 also shows the performance of a 2-D MMSE detection algorithm designed for a general 2-D ISI [11], [12]. The equalizer assumes that the inputs have a Gaussian distribution, which is an approximation. The 2-D MMSE equalizer as implemented here has infinite support.

B. Row-and-Column Detection Algorithm

Given the observation matrix $\mathbf{R}$, the calculation of the exact *a posteriori* probability (APP) of each element of the input matrix $\mathbf{X}$ is computationally intractable. However, the APP, $P(x_{i,j} =$

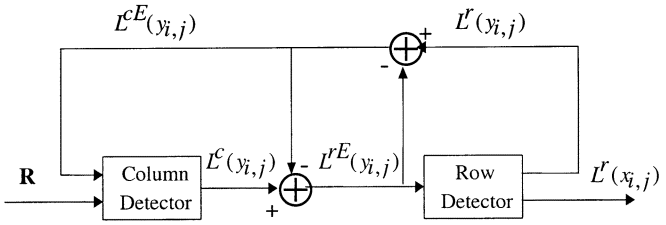

Fig. 4. Detector for the separable channel model shown in Fig. 1.

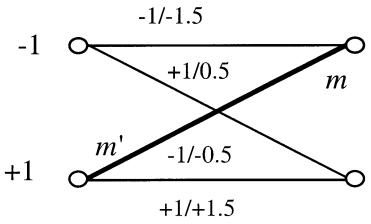

Fig. 5. Row ISI trellis.

$X \,|\, \mathbf{R}$), can be approximately calculated with an iterative detector. The structure of the iterative detector is shown in Fig. 4. In the following, we briefly describe the algorithms of the constituent column and row detectors in Fig. 4.

1) Column Detector: As mentioned before, the column ISI trellis is not binary. In fact, for an $L \times L$ ISI matrix, the number of inputs to the column ISI in Fig. 1 can be as many as 2^L. For the considered channel response, the row ISI output matrix $\mathbf{Y}$ has elements $y_{i,j} \in \{-1.5, -0.5, 0.5, 1.5\}$. Thus, the column ISI trellis has four states and four inputs corresponding to each state. Also, there are four branches arriving and departing from each state. The column detector takes a column of $\mathbf{R}$ and calculates the log-likelihood ratio (LLR) of each element of the corresponding column in matrix $\mathbf{Y}$. The MAP algorithm for a binary trellis [5], [10] can be extended to a MAP algorithm for nonbinary trellises [13]. Here, we give a brief description of the nonbinary MAP for the column ISI trellis. The LLR for $y_{i,j}$ is defined as

$$L^c(y_{i,j} = Y \,|\, \mathbf{R}_{:,\mathbf{j}}) = \log\left(\frac{P(y_{i,j} = Y \,|\, \mathbf{R}_{:,\mathbf{j}})}{P(y_{i,j} = -1.5 \,|\, \mathbf{R}_{:,\mathbf{j}})}\right) = \log \frac{\sum_{\substack{(s',s) \\ y_{i,j}=Y}} p(s', s, \mathbf{R}_{:,\mathbf{j}})}{\sum_{\substack{(s',s) \\ y_{i,j}=-1.5}} p(s', s, \mathbf{R}_{:,\mathbf{j}})} \quad (4)$$

where $\mathbf{R}_{:,\mathbf{j}}$ represents the jth column of the observation matrix, s' and s represent the starting state and the ending state of a branch of the column ISI trellis, respectively. In this section, we use the superscript "c" to represent the information produced or used by the column detector, and similarly define the symbol "r" for rows. Obviously, $L^c(y_{i,j} = -1.5 \,|\, \mathbf{R}_{:,\mathbf{j}})$ always equals zero. The choice of the base -1.5 is arbitrary. In (4), the joint probability $p(s', s, \mathbf{R}_{:,\mathbf{j}})$ consists of three terms [10]

$$p(s', s, \mathbf{R}_{:,\mathbf{j}}) = \alpha^c_{k-1}(s') \cdot \gamma^c_k(s', s) \cdot \beta^c_k(s). \quad (5)$$

The forward recursion is given by

$$\alpha^c_k(s) = \sum_{s'} \gamma^c_k(s', s) \cdot \alpha^c_{k-1}(s'). \quad (6)$$

The backward recursion is given by

$$\beta^c_k(s') = \sum_{s} \gamma^c_{k+1}(s', s) \cdot \beta^c_{k+1}(s). \quad (7)$$

The branch transition probability for the column ISI trellis $\gamma^c_k(s', s)$ is calculated using the extrinsic information provided by the row detector

$$\gamma^c_k(s', s) = p(r_{i,j} \,|\, y_{i,j} = Y) \cdot \exp(L^{cE}(y_{i,j} = Y)). \quad (8)$$

Here, the superscript "E" is used to represent extrinsic information. For the first iteration, there is no information available from the row detector; hence, $L^{cE}(y_{i,j} = Y)$ is initialized to zero. This follows from the assumption that the four input symbols to the column detector are equiprobable. After computing the column LLR defined in (4), the extrinsic information

$$L^{rE}(y_{i,j} = Y) = L^c(y_{i,j} = Y \,|\, \mathbf{R}_{:,\mathbf{j}}) - L^{cE}(y_{i,j} = Y) \quad (9)$$

is passed to the constituent row detector (Fig. 4).

2) Row Detector: The inputs to the row ISI are $x_{i,j} \in \{\pm 1\}$. The task of the row detector is to calculate the LLR of the row ISI input symbols

$$L^r(x_{i,j}) = \log \frac{P\left(x_{i,j} = +1 \,\middle|\, \mathbf{L}^{r\mathbf{E}}_{\mathbf{i},:}\right)}{P\left(x_{i,j} = -1 \,\middle|\, \mathbf{L}^{r\mathbf{E}}_{\mathbf{i},:}\right)} = \log \frac{\sum_{\substack{(m',m) \\ x_{i,j}=+1}} p\left(m', m, \mathbf{L}^{r\mathbf{E}}_{\mathbf{i},:}\right)}{\sum_{\substack{(m',m) \\ x_{i,j}=-1}} p\left(m', m, \mathbf{L}^{r\mathbf{E}}_{\mathbf{i},:}\right)} \quad (10)$$

and the LLR of the row ISI output symbols

$$L^r\left(y_{i,j} = Y \,\middle|\, \mathbf{L}^{r\mathbf{E}}_{\mathbf{i},:}\right) = \log\left(\frac{P\left(y_{i,j} = Y \,\middle|\, \mathbf{L}^{r\mathbf{E}}_{\mathbf{i},:}\right)}{P\left(y_{i,j} = -1.5 \,\middle|\, \mathbf{L}^{r\mathbf{E}}_{\mathbf{i},:}\right)}\right) = \log \frac{\sum_{\substack{(m',m) \\ y_{i,j}=Y}} p\left(m', m, \mathbf{L}^{r\mathbf{E}}_{\mathbf{i},:}\right)}{\sum_{\substack{(m',m) \\ y_{i,j}=-1.5}} p\left(m', m, \mathbf{L}^{r\mathbf{E}}_{\mathbf{i},:}\right)} \quad (11)$$

where $\mathbf{L}^{r\mathbf{E}}_{\mathbf{i},:}$ represents the extrinsic information for the ith row given by (9), and m' and m represent the starting state and the ending state of a branch of the row ISI trellis, respectively. In this case, we directly apply the Bahl–Cocke–Jelinek–Raviv (BCJR) algorithm to the binary row ISI trellis (Fig. 5). In (10) and (11), the value of $p(m', m, \mathbf{L}^{r\mathbf{E}}_{\mathbf{i},:})$ can be calculated using the BCJR algorithm. It is necessary to modify the calculation of the branch transition probability $\gamma^r_k(m', m)$ of the row ISI trellis due to the fact that there is no direct observation of the row ISI output. The modification is to calculate the branch transition probability of the row ISI trellis solely based on the extrinsic information obtained from the column detector. For example, for the labeled trellis branch (m', m) in Fig. 5

$$\gamma^r_k(m', m) = \frac{\exp(L^{rE}(y_{i,j} = -0.5))}{\sum_{Y \in \{-1.5, -0.5, 0.5, 1.5\}} \exp(L^{rE}(y_{i,j} = Y))} \quad (12)$$

where $L^{rE}(y_{i,j} = Y)$ is given by (9).

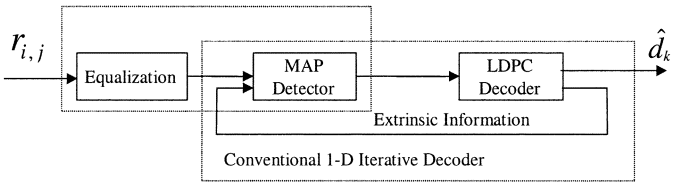

Fig. 6. Using equalization to reduce 2-D ISI into 1-D ISI.

The detection is performed iteratively between the column detector and the row detector. The information passed from the row detector to the column detector is the difference of (11) and (9)

$$L^{cE}(y_{i,j}=Y)=L^{r}\left(y_{i,j}=Y \mid \mathbf{L}^{r\mathbf{E}}_{\mathbf{i},:}\right)-L^{rE}(y_{i,j}=Y). \tag{13}$$

Once a predefined number of iterations are performed, (10) gives the LLR of the channel input symbols. The performance of this channel detector after one iteration is shown in Fig. 3 (named row-and-column).

IV. Iterative Decoding for 2-D ISI Systems

In this section, we describe two iterative decoding schemes for the system considered in Fig. 2 using the detection schemes described in the previous section and LDPC codes for error correction. We also briefly describe the "full graph" algorithm [11], [12], which is a scheme for joint equalization and decoding for a general 2-D ISI. In the next section, we compare the performance of the full graph algorithm with the schemes for a separable 2-D ISI to illustrate their superior performance.

A. Using the Combination of Equalization and MAP Approach

For the system shown in Fig. 2, the diagram of an iterative decoder is shown in Fig. 6. The equalizer performs equalization in the row dimension. For this scheme, iterations are performed between the column MAP detector and the LDPC decoder. The equalizer does not join the iteration process. We observe that the iterative decoder is a 2-D version of turbo equalization schemes for 1-D ISI channels [14].

B. Using the Row-and-Column Detection Algorithm

The iterative decoder using the row-and-column detection scheme is shown in Fig. 7. Every iteration in this scheme consists of two types of subiterations. The type-I subiteration is performed between the column detector and the row detector. After a fixed number of these subiterations, the row detector passes its extrinsic information to the LDPC decoder, starting the type-II subiteration, which is performed between the row detector and the LDPC decoder. The LDPC decoder uses the information passed to it by the row detector to calculate the *pseudo-posteriori* probabilities of the codeword bits, which are then passed back to the row detector. The second iteration then starts with the row detector using these probabilities as prior information and performing its subiterations (type-I) with the column detector. This process continues until a predefined number of iterations are exhausted.

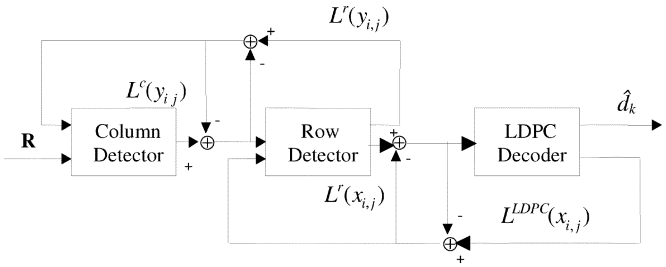

Fig. 7. This iterative detector consists of three concatenated constituent decoder/detectors.

In Fig. 7, we see that the row detector is connected to both the column detector and the LDPC decoder. So we consider the information obtained from both the column detector and the LDPC decoder in calculating the branch transition probability, $\gamma_k^r(m',m)$, for the row ISI trellis. Assuming that the column detector and the LDPC decoder make independent decisions, we have

$$\gamma_k^r(m',m)=\left(\frac{\exp(L^{rE}(y_{i,j}=-0.5))}{\sum_{Y\in\{-1.5,-0.5,0.5,1.5\}}\exp(L^{rE}(y_{i,j}=Y))}\right)\cdot\left(\frac{\exp(L^{\mathrm{LDPC}}(x_{i,j}=-1))}{\sum_{X\in\{-1,1\}}\exp(L^{\mathrm{LDPC}}(x_{i,j}=X))}\right) \tag{14}$$

for the labeled branch in Fig. 5. Here, $L^{\mathrm{LDPC}}(x_{i,j}=X)$ is the extrinsic information provided by the LDPC decoder to the row detector.

We also study the performance of the aforementioned decoding scheme when only the type-II subiteration, between the row detector and LDPC decoder, is performed. This alternative schedule is considered because the number of input symbols to the column detector increases exponentially with the row ISI length, which significantly increases the number of computations performed by it. Therefore, in this alternative scheme, only one column detection is performed after which the 2-D ISI is treated as a 1-D ISI.

C. Full Graph Message-Passing Algorithm

The full graph algorithm uses message passing to perform joint equalization and decoding for 2-D ISI. The message passing is performed on the joint three-level graph of the LDPC code and the channel ISI. The LDPC code graph, which forms the upper two levels, is a bipartite graph depicting how the codeword bit nodes are connected to the check nodes. The lower two levels are the channel ISI graph showing how the ISI induces dependencies among the codeword bits. The algorithm first performs a fixed number of iterations on the LDPC code bipartite graph. If decoding fails, then message passing is performed on the three-level graph for a fixed number of iterations.

The message-passing schedule per iteration for the three-level graph is as follows: codeword bit nodes $(x_{i,j})$ to observed data nodes $(r_{i,j})$; observed data nodes to codeword bit nodes; codeword bit nodes to check nodes; and finally, check nodes to codeword bit nodes.

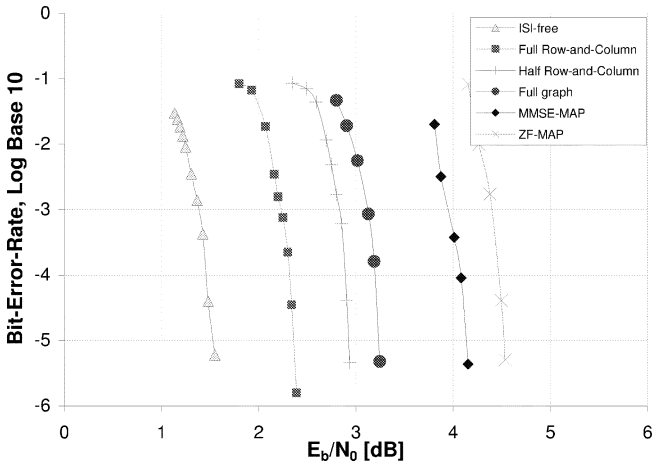

Fig. 8. BER performance of the iterative decoding schemes.

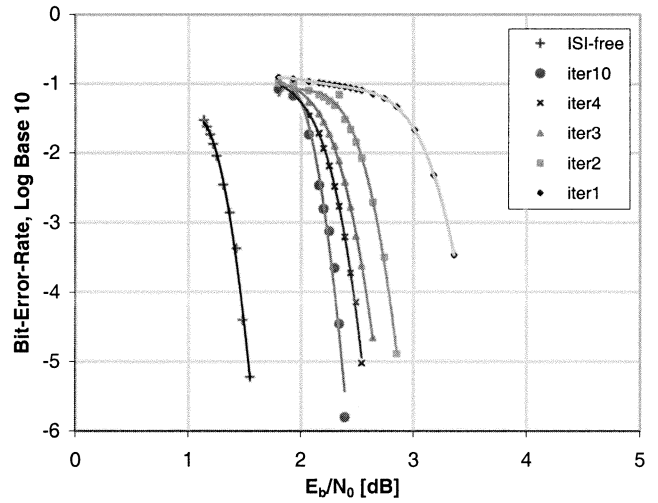

Fig. 9. BER performance of the full row-and-column decoding scheme for varying number of iterations.

V. Simulation Results

The performance of the decoding schemes described in Section IV is shown in Fig. 8. The ECC used is a block length 10 000, regular (3, 6) LDPC code [15]. The first curve from the left is the bit-error-rate (BER) performance of the LDPC code on the AWGN channel. The LDPC decoder performs a maximum of 50 iterations. All decoding performances will be compared to this curve.

The second curve from the left, named "full row-and-column," is the performance of the scheme described in Section IV-B. During the simulation, two type-I subiterations and one type-II subiteration are performed for each iteration. The curve shows the performance of this scheme after ten iterations. This scheme outperforms the "full graph" scheme (fourth curve from the left) by almost 1 dB. For the full graph algorithm, 20 iterations are performed on the LDPC code bipartite graph, and if decoding fails, then 50 iterations are done on the three-level graph using the schedule mentioned in Section IV-C. Fig. 9 shows the performance for varying the number of iterations for the full row-and-column decoding scheme.

The performance of the case when only the type-II subiterations are performed is also studied. The third curve from the left in Fig. 8, named "half row-and-column," shows the performance after five iterations. With more iterations, no performance improvement was observed.

The row-and-column and the full graph decoding schemes have a linear complexity in the code block length. However, the full graph algorithm has a computational complexity exponential in L^2 for an $L \times L$ ISI matrix, whereas for the row-and-column method it is exponential in L. Thus, we obtain not only improved performance but at a lower cost also.

The fifth curve from the left is the performance after ten iterations of the equalization and MAP approach using MMSE equalization. The equalizer used for the simulation has seven taps [16]. The sixth curve from the left is the performance after ten iterations when a ZF criterion is used for equalization. The performance is worse than the MMSE equalizer case because the ZF equalizer causes more noise correlation than the MMSE equalizer. In each case, the LDPC decoder performs 20 iterations after every MAP equalization.

VI. Conclusion

We have introduced two detection methods for uncoded separable 2-D ISI channels. These methods are able to generate soft decisions and, therefore, are suitable for iterative decoding with error correction codes. We also studied two iterative decoding schemes using these detection methods with LDPC codes. The best decoding performance is achieved using the row-and-column detection method, which employs modified MAP detectors for the ISI in each dimension. This method outperforms the full graph algorithm developed for a general 2-D ISI [12] for the separable channel response considered. The computational complexity of the row-and-column method is exponential in the channel response length in either dimension. This motivates equalizing a general 2-D ISI channel response to a nearby separable matrix, then applying the iterative decoding methods described here.

References

[1] K. M. Chugg, X. Chen, and M. A. Neifeld, "Two-dimensional equalization in coherent and incoherent page-oriented optical memory," *J. Opt. Soc. Amer. A*, vol. 16, pp. 549–562, Mar. 1999.

[2] X. Chen, K. M. Chugg, and M. A. Neifeld, "Near-optimal parallel distributed data detection for page-oriented optical memories," *IEEE J. Select. Topics Quantum Electron.*, vol. 4, pp. 866–879, Sept./Oct. 1998.

[3] R. Krishnamoorthi, "Two-dimensional Viterbi like algorithms," M.S. thesis, Univ. Illinois at Urbana-Champaign, 1998.

[4] W. Weeks IV, "Full surface data storage," Ph.D. dissertation, Univ. Illinois at Urbana-Champaign, 2000.

[5] L. R. Bahl, J. Cocke, F. Jelinek, and J. Raviv, "Optimal decoding of linear codes for minimizing symbol error rate," *IEEE Trans. Inform. Theory*, vol. IT-20, pp. 284–287, Sept. 1974.

[6] S. Benedetto, D. Divsalar, G. Montorsi, and F. Pollara, "Serial concatenation of interleaved codes: Performance analysis, design, and iterative decoding," *IEEE Trans. Inform. Theory*, vol. 44, pp. 909–926, May 1998.

[7] D. J. Mapps, T. Donnelly, P. J. Davey, and D. F. Smith, "Signal processing for present and future magnetic recording systems," *J. Magn. Soc. Jpn.*, vol. 21, pp. 211–220, Oct. 1997. Suppl. S2.

[8] A. Kikawada, N. Honda, and K. Ouchi, "A multi-track coding scheme designed for perpendicular recording using double layer medium and MR head," *J. Magn. Soc. Jpn.*, vol. 21, pp. 415–418, Oct. 1997. Suppl. S2.

[9] A. Kavčić, X. Ma, and M. Mitzenmacher, "Binary intersymbol interference channels: Gallager codes, density evolution, and code performance bounds," *IEEE Trans. Inform. Theory*, to be published.

[10] J. Hagenauer, "The turbo principle: Tutorial introduction and state of the art," in *Int. Symp. Turbo Codes*, Sept. 1997, pp. 1–11.
[11] J. A. O'Sullivan, N. Singla, Y. Wu, and R. S. Indeck, "Iterative decoding for two-dimensional intersymbol interference channels," in *Proc. Int. Symp. Information Theory*, Lausanne, Switzerland, July 2002, p. 198.
[12] N. Singla, J. A. O'Sullivan, R. S. Indeck, and Y. Wu, "Iterative decoding and equalization for 2-D recording channels," *IEEE Trans. Magn.*, vol. 38, pp. 2328–2330, Sept. 2002.
[13] J. Berkmann, "On turbo decoding of nonbinary codes," *IEEE Commun. Lett.*, vol. 2, pp. 94–96, Apr. 1998.
[14] M. Tüchler, R. Koetter, and A. Singer, "Turbo equalization: Principles and new results," *IEEE Trans. Commun.*, vol. 50, pp. 754–767, May 2002.
[15] D. J. C. MacKay, "Good error correcting codes based on very sparse matrices," *IEEE Trans. Inform. Theory*, vol. 45, pp. 399–431, Mar. 1999.
[16] N. Al-Dhahir and J. Cioffi, "Efficiently computed reduced-parameter input-aided MMSE equalizers for ML detection: A unified approach," *IEEE Trans. Inform. Theory*, vol. 42, pp. 903–915, May 1996.

Yunxiang Wu received the B.S. and M.S. degrees in electrical engineering from Beijing University of Posts and Telecommunications, Beijing, China, in 1988 and 1991, respectively, and the Ph.D. degree in electrical engineering from the University of Oklahoma, Norman, in 2000.

He joined Seagate Technology as a Research Staff Member in 2000. In 2001, he joined the Electrical Engineering Department at Washington University, St. Louis, MO, as a Visiting Researcher. Currently, he is a Senior Engineer at Samsung Information Systems America, Inc., San Jose, CA. His research interests include magnetic recording, digital communications, and signal processing.

Joseph A. O'Sullivan (S'83–M'85–SM'92–F'02) received the B.S., M.S., and Ph.D. degrees, all in electrical engineering, from the University of Notre Dame, Notre Dame, IN, in 1982, 1984, and 1986, respectively.

In 1986, he joined the faculty of the Department of Electrical Engineering at Washington University, St. Louis, MO, where he is now a Professor. He has joint appointments in the Departments of Radiology and Biomedical Engineering. He was a founding member and is now Director of the Electronic Systems and Signals Research Laboratory. He is Associate Director of the Center for Security Technologies at Washington University. He is Chair of the Faculty Senate, Chair of the Faculty Senate Council, and Faculty Representative to the Board of Trustees at Washington University. He was Secretary of the Faculty Senate and of the Senate Council from 1995 to 1998. His research interests include information theory, information-theoretic imaging, automatic target recognition, CT imaging in the presence of known high-density attenuators, information hiding, and hyperspectral imaging.

Prof. O'Sullivan is a member of Eta Kappa Nu, SPIE, SIAM, and AAAS. He was awarded an IEEE Third Millennium Medal. He was Co-Chair of the 1999 Information Theory Workshop on Detection, Estimation, Classification, and Imaging. He is Local Arrangements Chair for the 2003 IEEE Statistical Signal Processing Workshop. He was Chair of the St. Louis Section of the IEEE in 1994. He was the Publications Editor for the IEEE TRANSACTIONS ON INFORMATION THEORY from 1992 to 1995, was Associate Editor for Detection and Estimation, and was a Guest Associate Editor for the 2000 Special Issue on Information Theoretic Imaging.

Naveen Singla (S'00) received the B.Tech. degree in electrical engineering from the Indian Institute of Technology, Delhi, India, in 2000. Currently, he is working toward the Ph.D. degree in electrical engineering at Washington University, St. Louis, MO.

His research interests include information theory, magnetic recording, and coding theory.

Ronald S. Indeck (S'83–M'85–SM'92–F'02) received the B.S.E.E., M.S.E.E., and Ph.D. degrees from the University of Minnesota, Minneapolis.

He was a National Science Foundation Research Fellow at Tohoku University, Sendai, Japan. Since 1988, he has been with the Department of Electrical Engineering at Washington University, St. Louis, MO, where he is the Das Family Distinguished Professor and Director of the Center for Security Technologies. He has published more than 40 peer reviewed technical papers and been awarded more than a dozen patents. He is experienced in magnetic measurements and modeling, physical security and authentication, and currently leads research in projects of recording physics, magnetic devices, authentication, and exploiting massive databases.

Dr. Indeck is a member of the American Physical Society. He has received many awards, including the NSF Presidential Young Investigator Award from President Bush, the IBM Faculty Development Award, the Washington University Distinguished Faculty Award, the IEEE Centennial Key to the Future Award, and the IEEE Young Professional Award. He has served on many local committees and group activities, chaired sessions, and served several international conferences including General Chairman for International Magnetics Conference. He was an Editor for the IEEE TRANSACTIONS on MAGNETICS, and is President of the IEEE Magnetics Society.